# Core Design of 3.5 MWth Heat Pipe-Cooled Microreactor Using TRISO Fuel

Dongkyeong Lee [a] and Hyung Jin Shim [a*]
*[a]Seoul National University, 1 Gwanak-ro, Gwanak-gu, Seoul 08826, Republic of Korea*
*[*]Corresponding author: shimhj@snu.ac.kr*

***Keywords :* Reactor Core Design, Heat Pipe Cooled Reactor, Microreactor, TRISO, Reactor Physics**

## 1. Introduction

Microreactors are emerging as next-generation nuclear systems capable of providing reliable power and heat to remote and off-grid regions where large-scale plants and fossil fuel generators are often impractical. Owing to their compact size, inherent safety characteristics, and extended refueling intervals, they are well suited for specialized applications such as space missions, military operations, and deployment in extreme environments.

Recent research [1] has particularly emphasized the development of heat pipe–cooled microreactors. Conceptual design studies at the megawatt power level [2] have demonstrated not only their technical feasibility but also their scalability and applicability in demanding environments, underscoring their role as candidates for advanced microreactor systems. Furthermore, Westinghouse's eVinci™ [3] project highlights their commercialization potential by progressing from conceptual feasibility toward practical deployment, featuring passive cooling, modular transportability, and regulatory readiness for remote applications.

Motivated by these preceding studies, this study proposes a conceptual design of a 3.5 MWth hexagonal prism–type heat pipe–cooled microreactor that adopts fuel compacts containing TRISO particles in conjunction with sodium heat pipes. Neutronic parameters, such as excess reactivity, cycle length, power distribution, and temperature feedback, are considered to evaluate the feasibility and performance of the proposed configuration.

## 2. Core Design

### *2.1 Computational code and methodology*

The core is modeled and analyzed using McCARD, a Monte Carlo neutron-photon transport code developed at Seoul National University [4], with the ENDF/B-VII.1 nuclear data library [5]. The TRISO particle fuel is modeled using the FCEL functionality of McCARD, while the double-heterogeneous structure is treated with the Reactivity-equivalent Physical Transformation (RPT) method [6] to ensure computational efficiency and accuracy.

### *2.2 TRISO fuel and heat pipe*

In this study, the UCO-based TRISO fuel developed under the AGR program of the U.S. DOE is used as a reference, and the AGR program specification is applied to ensure long-term operation and adequate safety margins [7]. The detailed fuel parameters are summarized in Table I. A key modification in this design is the enlargement of the fuel compact radius from 0.615 cm to 0.975 cm. By maintaining the same packing fraction, this adjustment allows each compact to accommodate a larger number of TRISO particles, thereby increasing the overall uranium loading.

Table I: Fuel specifications

| **TRISO (packing fraction : 40%)** | | | |
|---|---|---|---|
| Parameters | Material | Radius[cm] (Thickness) | Density [g/cm3] |
| Kernel | UCO | 0.02125 | 11.05 |
| Buffer | Carbon | 0.03125 | 1.05 |
| Inner PyC | Carbon | 0.03525 | 1.90 |
| SiC | SiC | 0.03875 | 3.195 |
| Outer PyC | Carbon | 0.04275 | 1.90 |
| **Fuel Compact** | | | |
| Parameters | | Value | |
| Matrix material | | Graphite | |
| Fuel compact radius | | 0.975 cm | |
| Fuel pin hole radius | | 1.0 cm | |
| Fuel compact height | | 2.5 cm | |
| Number of fuel compacts per hole | | 50 | |

As shown in Table II, the specifications of the heat pipes are referenced from the Monolithic Heat Pipe Microreactor Reference Model [8]. According to this reference, the heat removal capacity of a single heat pipe is approximately 17 kW, which could support a total reactor thermal power of about 15 MWth. In this study, however, a more conservative design basis is adopted, assuming possible fabrication tolerances, additional thermal resistance, and the potential for localized hot spots under off-normal conditions. Accordingly, the heat removal capacity per heat pipe is limited to 10 kW, and the total core thermal power is set to 3.5 MWth. This conservative approach provides safety margins by accounting for uncertainties between theoretical performance and actual operating conditions.

Table II: Heat pipe specifications

| Parameters | Value |
|---|---|
| Working fluid | Sodium |
| Wick material | SS316 |
| Cladding material | SS316 |
| Heat pipe hole radius [cm] | 1.07 |
| Outer envelope radius [cm] | 1.05 |
| Inner envelope radius [cm] | 0.97 |
| Outer wick radius [cm] | 0.90 |
| Inner wick radius [cm] | 0.80 |
| Pore radius [cm] | 1E-6 |
| Wick porosity | 0.7 |
| Heat removal capacity* [kW/pipe] | 10 |
| Length (evap. / adiab. / cond.) [m] | 2.05  0.15 / 1.8 |

* Heat removal capacity conservatively set to 10 kW/pipe (Ref. [8] : 17 kW).

### *2.3 Fuel block design*

The core is composed of 55 hexagonal fuel blocks, each embedding fuel compacts together with heat pipes to enable passive cooling. A total of 378 heat pipes are incorporated to ensure conservative operation and provide adequate margin for reliable long-term performance. The blocks are classified into two types depending on the accommodation of shutdown rods, as illustrated in Fig. 1.

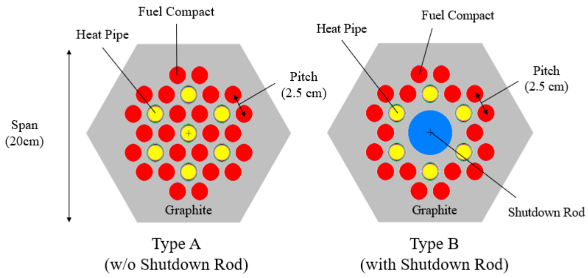


Fig. 1. Configuration of fuel block

A distinctive design feature is the concentration of fuel pins toward the block center with a minimized pitch, which enhances neutronic efficiency while simultaneously improving thermal management. To determine the optimal pin pitch and block span, single block neutronic calculations are performed under fixed uranium loading and moderator inventory. As shown in Fig. 2, $k_{inf.}$ increases with decreasing pin pitch across all span conditions. Fig. 3 compares representative pitches of 2.5 cm and 3.0 cm for varying spans, confirming that a span of 20 cm corresponds to an under-moderated regime. Based on these results, and considering mechanical and structural constraints, the fuel block design adopts a pin pitch of 2.5 cm and a span of 20 cm. This configuration provides sufficient reactivity while limiting the overall core size, consistent with the design strategy of central fuel pin concentration. The corresponding layouts for the 2.5 cm and 3.0 cm cases are presented in Fig. 4, and the final block specifications are summarized in Table III.

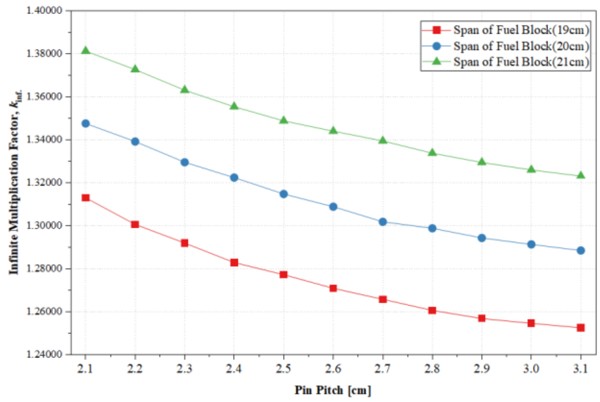


Fig. 2. Variation of $k_{inf.}$ with pin pitch for different span

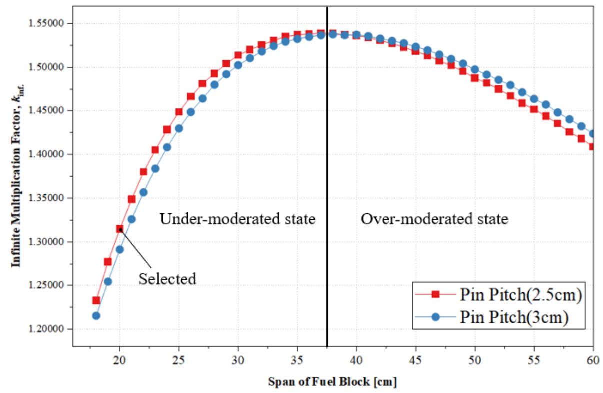


Fig. 3. Comparison of $k_{inf.}$ between 2.5 cm and 3.0 cm pin pitch across different span lengths

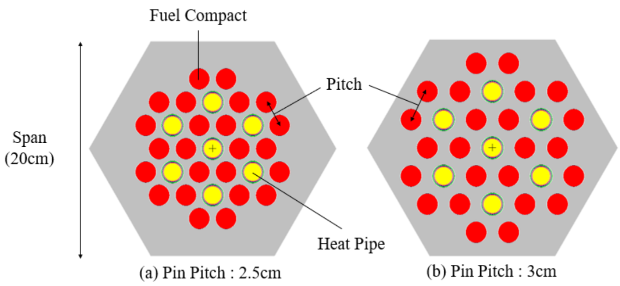


Fig. 4. Fuel block configurations with pin pitches of 2.5 cm and 3 cm

Table III: Fuel block (w/o shutdown rod) specifications

| Parameters | Value |
|---|---|
| Span of Fuel Block | 20 cm |
| Pin pitch | 2.5 cm |
| Fuel compact hole radius | 1 cm |
| Heat pipe hole radius | 1.07 cm |
| Shutdown rod hole radius | 2.5 cm |
| Number of fuel pin | 24 |
| Number of heat pipe | 7 |
| Mass of uranium per fuel block | 5.235 kg |

### *2.4 Core design*

Table IV summarizes the design parameters of the proposed microreactor. The core consists of 55 hexagonal fuel blocks, each containing fuel compacts with TRISO particles and integrated heat pipes for passive heat removal. In addition, control drums are incorporated in the radial reflector region to provide reactivity control, as illustrated in Fig. 5 and Fig. 6.

Table IV: Design parameters of the core

| Parameters | Value |
|---|---|
| Reactor type | Heat Pipe Cooled Reactor |
| Thermal power | 3.5 MWth |
| Core(active) height | 260(150) cm |
| Refueling cycle | 6 years |
| Core diameter | 250 cm |
| Fuel material | TRISO (UCO kernel) |
| Uranium enrichment | 15.5 wt.% |
| Packing fraction | 40% |
| Uranium mass | 278.8 kg |
| Number of fuel blocks | 55 |
| Number of fuel pins | 1,278 |
| Number of heat pipes | 378 |
| Number of control drums | 18(Small :12, Large : 6) |
| Number of shutdown rods | 7 |
| Heat removal capacity | 10 kW/pipe |
| Heat pipe working fluid | Sodium |
| Fuel block material | Graphite |
| Reflector material | BeO |
| Control absorber material | $B_4C$ (90 wt.% $^{10}B$ enriched) |

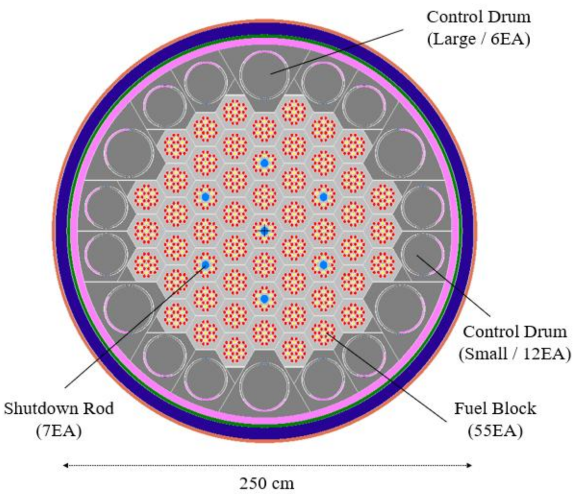


Fig. 5. Radial configuration of core

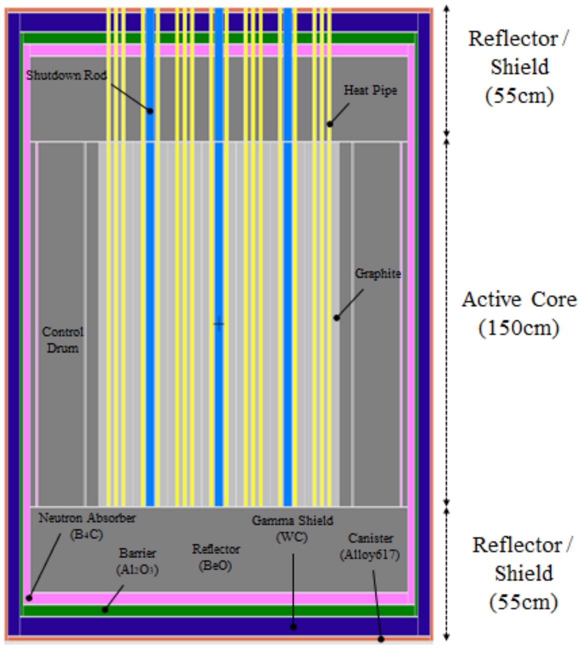


Fig. 6. Axial configuration of core

## 3. Results

### *3.1 Depletion calculation*

Depletion calculations are performed using McCARD with 10,000 histories per cycle, 150 inactive cycles, and 300 active cycles. Fig. 7 shows the variation of $k_{eff.}$ with burnup for pin pitches of 2.5 cm and 3.0 cm. Both configurations sustain criticality for approximately 2,190 EFPD, corresponding to a discharged burnup of about 27.5 MWd/kgU, with the 2.5 cm pitch maintaining consistently higher $k_{eff.}$ throughout the cycle. Accordingly, the 2.5 cm pitch is adopted as the reference configuration. In all calculations, the statistical uncertainty of $k_{eff.}$ remains below 0.00056. These results indicate that the core maintains criticality for 6 years of continuous operation without refueling while preserving an adequate reactivity margin over the cycle.

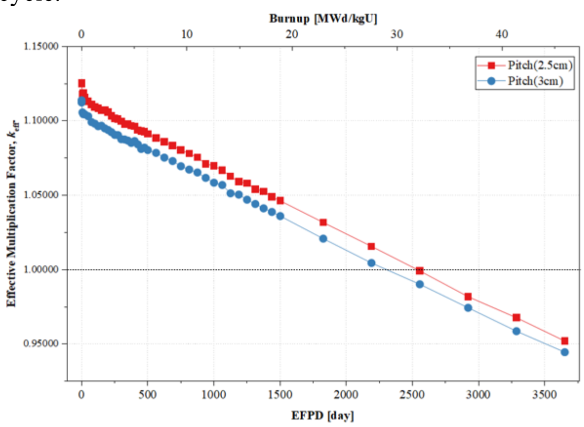


Fig. 7. $k_{eff.}$ vs. EFPD of calculated burnup results

The neutron flux spectra in the active core region exhibit predominantly thermal characteristics. As burnup progresses from BOC to EOC, the thermal neutron fraction increases, indicating a softening of the spectrum that supports sustained reactivity. This trend, illustrated in Fig. 8, highlights the role of spectral shift in promoting effective fuel utilization and consistent core performance over the cycle.

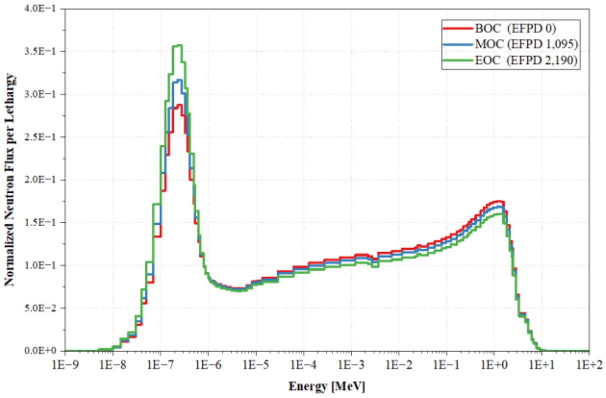


Fig. 8. Normalized neutron flux spectrum in the active core region

*3.2 Power distribution*

The radial power distribution on a fuel-block basis is shown in Fig. 9 for BOC, MOC, and EOC. At BOC, the highest block power appears not at the core center but in the adjacent region, and this trend persists through MOC and EOC. The maximum normalized block powers are 1.19 at BOC, 1.14 at MOC, and 1.10 at EOC.

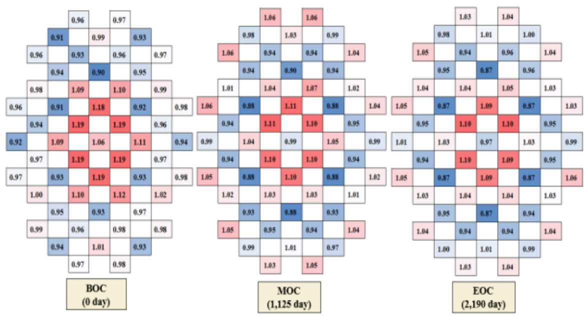


Fig. 9. Normalized radial power distribution

The axial power distribution exhibits a bottom-peaked profile consistently across BOC, MOC, and EOC, as shown in Fig. 10. This trend results from enhanced moderation near the lower reflector region, while reduced moderation in the upper part of the core, due to the presence of heat pipes and shutdown rods, reinforces the bottom-peaked shape. The axial peaking factor ($F_Z$) decreases gradually over the cycle, from 1.54 at BOC to 1.39 at EOC.

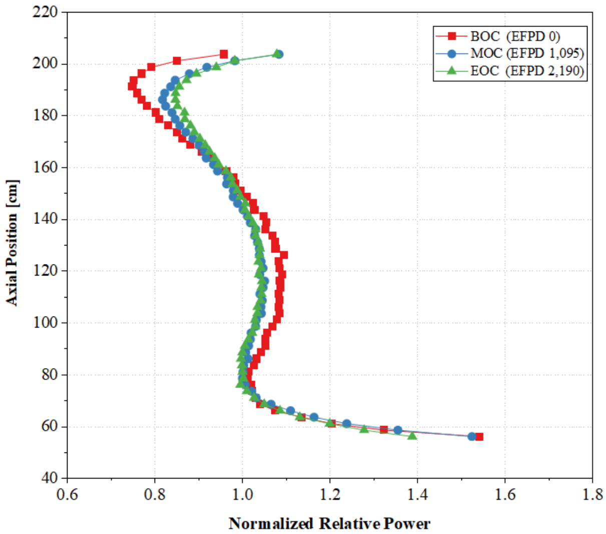


Fig. 10. Normalized axial power distribution

*3.3 Reactivity of control devices*

The reactor employs a dual reactivity control system composed of control drums and shutdown rods. A total of 18 control drums are installed in the reflector region and arranged into large and small groups to allow both coarse and fine adjustment during normal operation. Drum rotation provides continuous reactivity control with sufficient operational margin. Neutronic analysis shows that when all drums are rotated outward toward the reflector, $k_{eff.}$ reaches 1.12719 ± 0.00044, whereas full inward rotation reduces $k_{eff.}$ to 0.99603 ± 0.00045. These results, summarized in Table V and illustrated in Fig. 11.

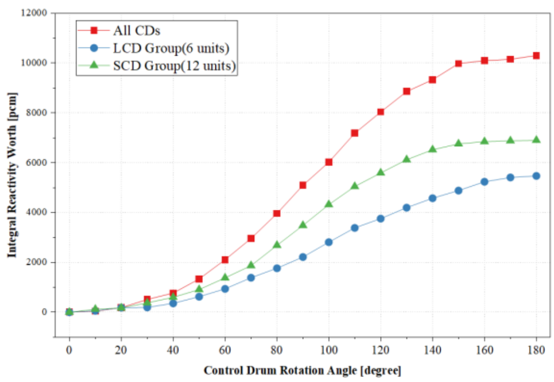


Fig. 11. Control drum reactivity worth

In addition, the shutdown rods are dedicated safety devices that ensure prompt reactor shutdown during emergency situations. A total of seven rods are positioned within selected fuel blocks, each with a diameter of 2.5 cm and composed of $B_4C$ enriched with 90 wt.% $^{10}B$. While withdrawn during normal operation, they provide substantial negative reactivity upon insertion, exceeding the capability of the control drums alone, as summarized in Table V.

Table V: Rod worth of the core

| Control Durum | Shutdown Rod | $k_{eff.}$(STD) | Reactivity(pcm) |
|---|---|---|---|
| All Out(180°) | Fully Withdrawn | 1.12719 (0.00044) | 11,284 |
| All Out(180°) | Fully Inserted w/o the Highest Reactivity Rod | 0.94098 (0.00045) | -6,272 |
| All Out(180°) | Fully Inserted | 0.91532 (0.00047) | -9,251 |
| All In(0°) | Fully Withdrawn | 0.99603 (0.00045) | -399 |
| All In(0°) | Fully Inserted w/o the Highest Reactivity Rod | 0.79274 (0.00048) | -26,145 |
| All In(0°) | Fully Inserted | 0.73540 (0.00046) | -35,980 |

### *3.4 Reactivity coefficients*

Reactivity coefficients are evaluated under BOC conditions using the direct subtraction method. The results for FTC, MTC, and ITC are summarized in Table VI. Across the temperature range of 300–1200 K, all coefficients show negative values, which demonstrates the inherent negative reactivity feedback of the core.

Table VI: Reactivity coefficients [pcm/K]

| Temperature | FTC | MTC | ITC |
|---|---|---|---|
| 300-600K | -4.63053 ± 0.06353 | -2.81091 ± 0.06576 | -3.63880 ± 0.06383 |
| 600-900K | -3.32484 ± 0.07004 | -1.73039 ± 0.06925 | -3.45637 ± 0.06675 |
| 900-1200K | -2.94536 ± 0.06974 | -3.45015 ± 0.07271 | -3.66279 ± 0.06959 |

## 4. Conclusions and future work

This study presents the conceptual design of a 3.5 MWth prismatic-type heat pipe–cooled microreactor that using UCO-based TRISO fuel. The design adopts a compact hexagonal block configuration with centrally concentrated fuel pins and minimized pitch, aiming to improve neutronic efficiency and facilitate effective heat transfer. Neutronic analysis with McCARD shows that the core sustains criticality for approximately 2,190 EFPD, achieving a burnup of 27.5 MWd/kgU, while maintaining acceptable power distributions, inherent negative reactivity feedback coefficients, and sufficient reactivity control capability. These results suggest that the proposed configuration may represent a viable option for reliable and long-lived power generation in specialized missions such as defense support, disaster response, space exploration, and deployment in remote areas.

Future work will extend this concept through detailed radiation shielding assessments, coupled neutronic–thermal hydraulic analyses, and optimization studies aimed at further compactness, thereby supporting the development of a long-lived and inherently safe microreactor design.

## REFERENCES

[1] YAN, Binghuo H.; WANG, Chenglong; LI, Liangguo G. The technology of micro heat pipe cooled reactor: A review. Annals of Nuclear Energy, 2020, 135: 106948.
[2] MCCLURE, Patrick Ray, et al. Design of megawatt power level heat pipe reactors. Los Alamos National Laboratory (LANL), Los Alamos, NM (United States), 2015.
[3] SWARTZ, Matt M., et al. Westinghouse eVinci™ heat pipe micro reactor technology development. In: International conference on nuclear engineering. American Society of Mechanical Engineers, 2021. p. V001T04A018.
[4] SHIM, Hyung-Jin, et al. McCARD: Monte Carlo code for advanced reactor design and analysis. Nuclear Engineering and Technology, 2012, 44.2: 161-176.
[5] CHADWICK, Mark B., et al. ENDF/B-VII. 1 nuclear data for science and technology: cross sections, covariances, fission product yields and decay data. Nuclear data sheets, 2011, 112.12: 2887-2996.
[6] KIM, Yong-Hee; KIM, Kang-Seog; NOH, Jae-Man. Reactivity-equivalent physical transformation for homogenization of double-heterogeneous fuels. In: Proceedings of the Korean Nuclear Society Conference. Korean Nuclear Society, 2005. p. 115-116.
[7] MARSHALL, Douglas. AGR-5/6/7 Fuel Specification. Idaho National Lab.(INL), Idaho Falls, ID (United States), 2017.
[8] ORTENSI, Javier, et al. The Monolithic Heat Pipe Microreactor Reference Plant Model. Idaho National Laboratory (INL), Idaho Falls, ID (United States), 2024.